One advantage of the method is that it examines a wider temperature range than does the isothermal kinetic method. Provided that the tests are sufficiently accurate, it is possible to detect any activation energy change.

Since three temperatures stages and three durations for each stage generally are considered as a minimum for isothermal kinetic studies, the nonisothermal method does not appear to offer any decisive advantage. The definitive need for more sophisticated equipment (temperature programmer, computer, and plotter) is a disadvantage. On the other hand, the nonisothermal method may lead to more precise results with less experimental effort, *e.g.*, data points. Furthermore, it requires only a fraction of the time an isothermal experiment does. Selection of a method depends on the equipment and the time available.

REFERENCES

(1) A. R. Rogers, *J. Pharm. Pharmacol.*, **15**, 101T (1975).

(2) S. P. Eriksen and H. Stelmach, *J. Pharm. Sci.*, **54**, 1029 (1965).

(3) M. A. Zoglio, J. J. Windheuser, R. Vatti, H. V. Maulding, S. S. Kornblum, A. Jacobs, and H. Hamot, *ibid.*, **57**, 2080 (1968).

Time and Temperature Dependence of Disintegration and Correlation between Dissolution and Disintegration Rate Constants

J. T. CARSTENSEN ˣ, ROHIT KOTHARI, V. K. PRASAD *, and JANE SHERIDAN ‡

Received June 25, 1979, from the *School of Pharmacy, University of Wisconsin, Madison, WI 53706.* Accepted for publication October 17, 1979.

*Biopharmaceutics Laboratory, Food and Drug Administration, Washington, D.C. ‡Hoffmann-La Roche Inc., Nutley, NJ 07110.

Abstract □ Commercial prednisone tablets were subjected to dissolution tests by USP basket and paddle methods. It was found experimentally that disintegration adheres to an exponential decay law: $\ln(W/W_0) = -d(t - t_i)$, where W is the nondisintegrated weight, d is a disintegration constant, t is time, and t_i is a lag time. Dissolution has been reported to adhere to a similar law, where the dissolution constant, K, follows a pseudo-Arrhenius relationship with changing temperature. Within a certain temperature range, this relationship also exists for the disintegration rate constant, d. A correlation exists in these tablets between K and d. The shaft length in the dissolution apparatus plays a part in the disintegration (and hence dissolution) rate and, therefore, is an important apparatus parameter affecting reproducibility.

Keyphrases □ Disintegration—commercial prednisone tablets, time and temperature dependence, correlation between dissolution and disintegration rate constants □ Prednisone—commercial tablets, time and temperature dependence of disintegration, correlation between dissolution and disintegration rate constants □ Dissolution—commercial prednisone tablets, time and temperature dependence of disintegration, correlation between dissolution and disintegration rate constants

Several recent articles correlated two- or three-component dissolution model parameters with those of disintegration in the same apparatus. These studies were aimed at elucidation of the type of dissolution curve obtained in dissolution experiments both for control and for research purposes. The curves usually are *s*-shaped. Wagner (1) and Wood (2) first recognized the importance of this type of curve, and a probit and a Weibul function were suggested later as a descriptive means (1–4).

Several investigators demonstrated that disintegration and dissolution in an apparatus can be correlated and that these factors lead to *s*-shaped curves (5–11). Carstensen *et al.* (7, 8) suggested that the best general trial function is one in which the weight of undisintegrated tablet is monitored as a function of time. The dimensions of the tablets remaining (such as thickness) as a function of time can be useful in certain cases; but since many tablets swell on contact with water, the functions become complicated. Furthermore, the thickness of a swelling, disintegrating tablet is difficult not only to monitor but also to define.

The simplest model of weight *versus* time that appears compatible with experimental data (8) is a simple exponential decay function. Double exponentials may apply in more complicated systems. This model has been recognized in compendial work, and disintegrating dissolution calibrators have been suggested. This article presents data showing the disintegration–dissolution behavior of a conventional prednisone tablet.

Excellent research and review articles regarding the mechanism of disintegration have been published (12–14), and the effect of temperature on dissolution has been elucidated (15). This article reports the dependence of tablet disintegration on temperature and also the effect of the length of the stirring shaft on dissolution.

EXPERIMENTAL

Commercial prednisone tablets were assayed and found to contain starch, lactose, metallic stearate, and prednisone. Two 20-mg tablets were placed in the basket of a USP basket dissolution apparatus in a thermostated bath. The apparatus was operated at 150 rpm. This agitation speed was chosen because problems with liquid homogeneity exist at lower rotational speeds (9). Samples were taken routinely at appropriate time intervals and, after filtration[1], were assayed using the spectrophotometric absorbance at 242 nm. The amount of prednisone then was determined by comparison with a standard curve of prednisone obtained with a USP reference standard. The experiment was repeated using a different shaft length (Fig. 1), *i.e.*, assembling the shaft onto the motor such that the length of free shaft was different from that first used. The two shaft "lengths" used are denoted as positions I and II (Fig. 1).

A set of experiments was performed (in both positions) to establish the disintegration rate of the tablets in the apparatus. These experiments were done as follows (6, 7). An experiment was carried out for t_i min and then was stopped. The basket was lifted out, and the tablets were removed and dried to constant weight, W, at 100°. This weight was compared with the weight, W_0, of a similarly dried tablet prior to the dissolution test. The experiment then was repeated for other t_i values.

The experiments were repeated using a USP paddle apparatus at 150 rpm. Experiments were carried out at 10, 20, and 30° for the paddle apparatus and at 0, 5, 10, 15, 20, 30, and 37° for the basket apparatus.

[1] Millipore filter.

0022-3549/80/0300-0290$01.00/0

Table I—Dissolution Constants and Disintegration Constants at Various Temperatures and Positions

Temperature	Position[a]	$10^5 K$, sec^{-1}	r^2	$10^3 d$, sec^{-1}	r^2
		Basket, 150 rpm			
0	I	8.3	0.99	2.7	0.98
0	II	8.3	0.99	2.8	0.99
5°	I	8.3	0.99	2.9	0.99
5°	II	8.7	0.996	3.5	0.998
10°	I	24.7	0.97	3.6	0.992
10°	II	28.1	0.98	4.1	0.98
15°	I	38.0	0.96	4.4	0.998
15°	II	38.3	0.96	4.9	0.99
20°	I	111	0.99	5.7	0.97
20°	II	125	0.97	6.7	0.95
30°	I	206	0.993	8.2	0.94
30°	II	248	0.996	8.7	0.90
37°	I	240	0.99	13.2	0.91
37°	II	284	0.992	14.6	0.96
		Paddle, 150 rpm			
10°	I	44.5	0.97	3.9	0.996
10°	II	58.9	0.97	4.0	0.99
20°	I	145	0.92	5.6	0.996
20°	II	164	0.96	7.0	0.97
30°	I	219	0.999	9.6	0.98
30°	II	228	0.97	9.7	0.96

[a] Positions I and II are 22 and 32 cm, respectively, and equal the shaft length.

RESULTS AND DISCUSSION

All dissolution and disintegration data show s-shaped curves as exemplified in Fig. 2. The data were recast in semilogarithmic form, and, as shown in Fig. 3 and Table I, follow the equations:

$$\ln(W/W_0) = -d(t - t_i) \quad \text{(Eq. 1)}$$

$$\ln(m/m_0) = -K(t - t_i') \quad \text{(Eq. 2)}$$

where m is the amount of undissolved drug, d is a disintegration rate constant ($time^{-1}$), K is a dissolution rate constant ($time^{-1}$), t_i and t_i' are lag times, and the subscript zero denotes zero time.

To present all of the data points graphically, they were converted to reduced parameters in the following fashion. The least-squares parameters d and t_i (and K and t_i') were calculated as shown in Table I. For disintegration, the experimental value of $\ln(W/W_0)$ at time $t^\dagger$ was used as the ordinate (y-axis) in Fig. 4. The corresponding abscissa value, x, then was obtained by inserting the $t^\dagger$ value and the least-squares values of d and t_i into $x = -d(t - t_i)$. A similar procedure was used for dissolution (Fig. 5).

This graphic method allows visualization of how all data points fit the two equations. Essentially straight lines of unit slope and zero intercept are obtained in Figs. 4 and 5. The graphical presentation is not statistical. Usual least-squares methods are not possible by the reduced presentation because both x and y have errors of comparable magnitude, and most methods addressing this situation fail when (as in the described treatment) the error on the y-axis is not independent of the error on the x-axis.

Statistical evidence is confined to comparison of the s_{yx}^2 values of the data treated according to Eq. 1 as compared to other functions, where s_{yx}^2 is the total sum of squares divided by the degrees of freedom ($n - 2$),

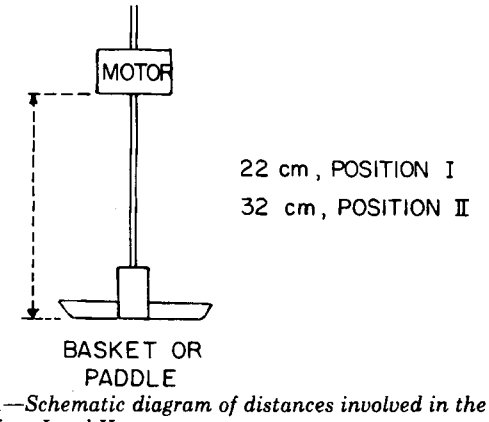

Figure 1—*Schematic diagram of distances involved in the assembly for positions I and II.*

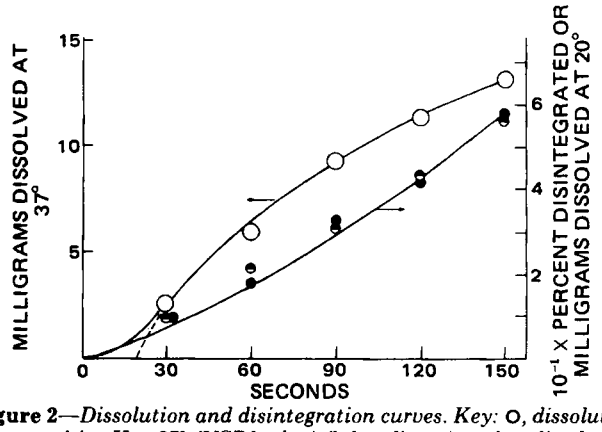

Figure 2—*Dissolution and disintegration curves. Key: ○, dissolution curve, position II at 37° (USP basket) (left ordinate); and ●, dissolution, and ◒, disintegration, at 20° (USP basket, position I) (right ordinate).*

where n is the number of experimental points. The data from the dissolution in USP basket position I at 15° are used as an example. Table II compares the data treated by Eq. 1 with the data treated by the function:

$$y = [1 - (W/W_0)] = (t/t_d)^n \quad \text{(Eq. 3a)}$$

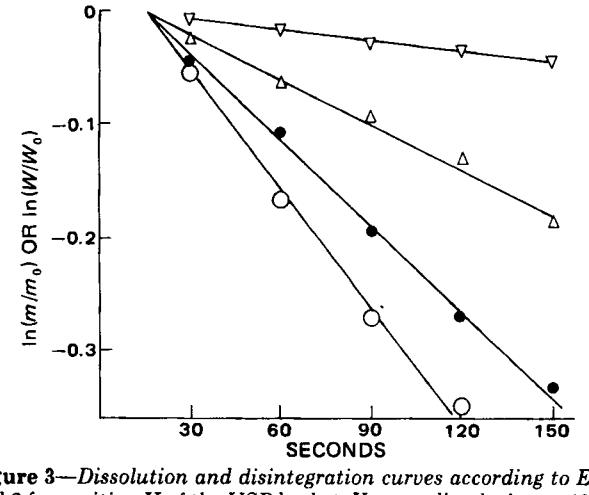

Figure 3—*Dissolution and disintegration curves according to Eqs. 1 and 2 for position II of the USP basket. Key: ▽, dissolution at 10°; △, dissolution at 20°; ●, dissolution at 30°; and ○, disintegration at 5°.*

Table II—Statistical Comparison for USP Basket (15°, Position I) Treated by Eq. 1 and by Eq. 3 as an Example

t, sec	ln t	100 y (Percent Dis-integrated)	$z_1 = \ln y$	$\bar{z}_1$	$\bar{y}_1$ × 100	Δ_1^2	$z_2 = \ln(1-y)$	$\bar{z}_2$	$\bar{y}_2$ × 100	Δ_2^2
30	3.4	7.9	−2.538	−2.500	8.2	0.09	−0.082	−0.076	7.3	0.36
60	4.09	18.2	−1.704	−1.746	17.5	1.69	−0.201	−0.207	18.7	0.25
90	4.50	28.9	−1.241	−1.298	27.3	2.56	−0.341	−0.339	27.7	1.44
120	4.79	36.8	−1.000	−0.982	37.5	0.49	−0.459	−0.470	37.5	1.69
150	5.01	45.7	−0.783	−0.742	47.6	1.21	−0.611	−0.602	45.2	0.25
						$\Sigma\Delta^2 = 6.04$				$\Sigma\Delta^2 = 3.99$
						$s_{yx}^2 = 2.01$				$s_{yx}^2 = 1.33$
				Slope		1.091				−0.0044
				Intercept		−6.209				0.056
				Correlation coefficient		−0.998				−0.999

which is the equation derived by Kitamori and Iga (11). In logarithmic form, this equation is:

$$z_1 = \ln[1 - (W/W_0)] = n \ln(t) - n \ln(t_d) \qquad \text{(Eq. 3}b\text{)}$$

where n is an equation parameter and t_d is the disintegration time. The least-squares fit for the data is $z_1 = 1.091 \ln t - 6.209$ ($r^2 = 0.996$), where r^2 is the square of the correlation coefficient.

The s_{yx}^2 values are obtained for Eq. 3a first by finding the line values, $\bar{z}_1$, corresponding to Eq. 3b for each t value and then by converting them to $\bar{y}_1$ values (percent disintegrated). These values are shown in Table II. A similar calculation is shown for the data plotted according to Eq. 1 [$z_2 = \ln(W/W_0)$ and $y_2 = 1 - (W/W_0)$]. The sums of squares were equally good whether obtained by Eq. 1 or by Eq. 2. The sums of squares obtained by Eq. 1 were always lower than those calculated from Eq. 3a but only by small amounts, and none of the s_{yx}^2 ratios exceeded the critical F values with (3,3) degrees of freedom.

The derivation of Eq. 3a (10) is based on an assumption (16) that the thickness of a tablet will decrease steadily as it disintegrates. This assumption usually is not the case since swelling initially will cause an increase in thickness. Even if the basis for the derivation of Eq. 3a may not be general, Eq. 3a as shown provides a good trial function. However, Eq. 1 will be used in the remainder of this article.

Correlation between Disintegration and Dissolution—The data in Table I concerning the values of K and d are plotted in Fig. 6. It is graphically evident that there is a correlation and that this correlation is not linear. Many curvilinear functions may fit this curve, one of which ($r = 0.97$) is $\ln[(300 - 10^5 k)] = -0.214 \times 10^3 d + 6.4$. This function is consistent with the theoretical models proposed elsewhere (5–8, 10). At high d values, K should become independent of d (7), and this result probably is the explanation for the curving off at high d values.

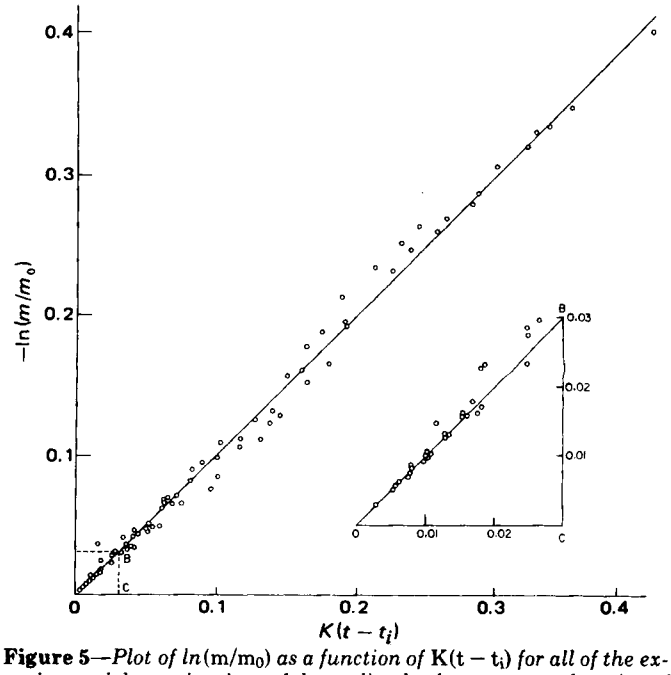

Figure 5—*Plot of* $\ln(m/m_0)$ *as a function of* $K(t - t_i)$ *for all of the experimental determinations of the undissolved amount as a function of time.*

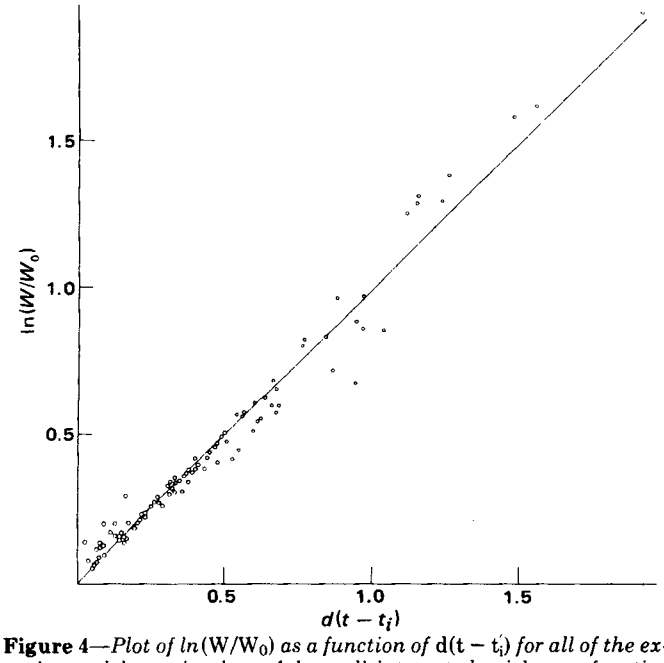

Figure 4—*Plot of* $\ln(W/W_0)$ *as a function of* $d(t - t_i)$ *for all of the experimental determinations of the undisintegrated weight as a function of* t.

Effect of Shaft Length—Table I shows that position II gave significantly ($p > 0.995$) higher results than did position I as far as both disintegration and dissolution are concerned. Since disintegration affects dissolution [$K = f(d)$], it is speculated that the change in disintegration is caused by the longer shaft length and that this effect is the cause for the observed differences.

Effect of Temperature—The logarithm of the disintegration constants, d, is plotted *versus* the reciprocal temperature in Fig. 7. The

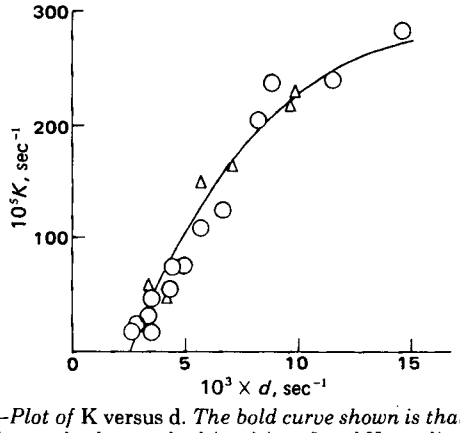

Figure 6—*Plot of* K versus d. *The bold curve shown is that expressed in Eq. 3. Key:* ○, *basket method (positions I and II not distinguished); and* △, *paddle method (positions I and II not distinguished).*

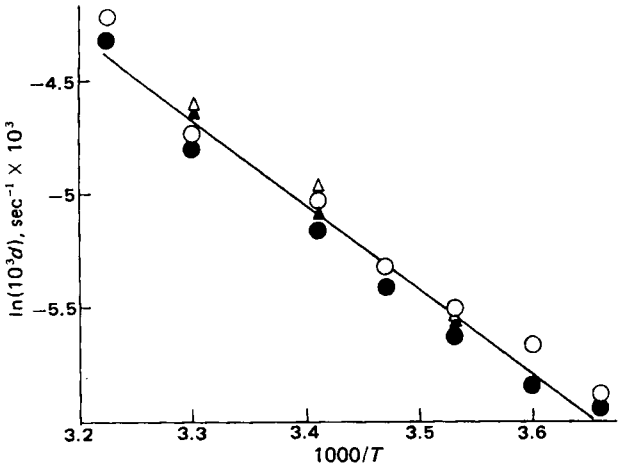

Figure 7—*Temperature dependence of the disintegration constant, d (seconds^{-1}). Key: O, USP basket method; and Δ, USP paddle method. Solid circles are position I, and open circles are position II.*

least-squares equation for the line is:

$$\ln d = -(7000/R)(1/T) - 0.0152 \quad \text{(Eq. 4)}$$

According to previous investigators (12–14), the disintegration of a tablet proceeds *via* two principal mechanisms: (*a*) penetration of liquid into the tablet pores, and (*b*) expansion of the disintegrant exposed in the pore walls. A large pore size facilitates penetration; but if it is too large, the expansion of the disintegrant will not cause sufficient strain to rupture the tablet (12, 17). Therefore, either mechanism or both simultaneously may be the rate-controlling step.

If the rate-controlling process is solely the penetration of pores of a radius *r*, then, as shown previously (12, 18, 19), the length of liquid penetration, *L*, into the capillaries is time dependent according to:

$$L^2 = (r\gamma \cos\theta)/(2\eta)t = q^2t \quad \text{(Eq. 5)}$$

where:

$$q = [r\gamma \cos\theta/(2\eta)]^{1/2} \quad \text{(Eq. 6)}$$

and where γ is the interfacial tension between the liquid and the solid, η is the viscosity, and θ is the contact angle.

If the amount penetrated disintegrates in a certain length of time, t^*, after the time of wetting and if the radius of the tablet is L_0 cm initially, then the weight remaining after t sec would be given by (20, 21):

$$W/W_0 = (L_0 - L)^3/L_0^3 \quad \text{(Eq. 7)}$$

Inserting Eq. 7 into Eq. 5 gives (21):

$$[1 - (W/W_0)^{1/3}]^2 = (q/L_0)^2(t - t^*) \quad \text{(Eq. 8)}$$

Data treated similarly are shown in Table III, and it is apparent that the equation does not hold. However, the model is simple, and more complicated relations could be visualized. But if *d*, the disintegration constant, is related more closely to the volume rate of penetration, then *d* would be expected to be linearly related to q^3, *i.e.*:

$$\ln d = 1.5 \ln(\gamma) + 1.5 \ln(\cos\theta) - 1.5 \ln(\eta) + Q \quad \text{(Eq. 9)}$$

where *Q* is a temperature-independent term.

Table III—Data from Table II Treated by Eq. 8

t, sec	100 (W/W_0), Experimental, %	$[1 - (W/W_0)^{1/3}]^2$	$\widetilde{100(W/W_0)}$, Predicted, %	Δ^2, %^{2}
30	92.1	0.00073	—[a]	—[a]
60	81.8	0.0042	78.7	9.6
90	71.1	0.0116	68.4	7.3
120	63.2	0.0201	61.5	2.9
150	54.3	0.0339	56.2	3.6
				$\Sigma\Delta^2 = 23.4$

[a] Least-squares parameters predicts a negative number for $[1 - (W/W_0)^{1/3}]^2$ at $t = 30$ sec. The least-squares fit was $[1 - (W/W_0)^{1/3}]^2 = 0.000274t - 0.01059$ with $r^2 = 0.95$ and $s^2_{yx} = 23.4/2 = 11.7\%^2$.

The dependence of θ on T is slight (22, 23) as shown. Stepanov *et al.* (24) gave θ values of water on sapphire of:

$$\theta = 8.8 + 8.2 \times 10^{-15}T^6 \quad \text{(Eq. 10)}$$

i.e., $\theta = 11.5$ [or $\ln(\cos\theta) = -0.0206$] at $T = 273°$ ($1/T = 0.00366$) and $\theta = 15.1$ [or $\ln(\cos\theta) = -0.0351$] at $T = 303°$ ($1/T = 0.00333$). On metals, θ decreased with temperature to the same extent (25). Linear Eq. 10 when expressed as $\ln(\cos\theta)$ as a function of $1/T$ is approximately as follows.

For sapphire:

$$\ln(\cos\theta) = 44(1/T) - 0.18 \quad \text{(Eq. 11}a\text{)}$$

For metals:

$$\ln(\cos\theta) = -44(1/T) + 0.13 \quad \text{(Eq. 11}b\text{)}$$

Hence, the activation energy, *E*, is negligible (-88 cal/mole $< E <$ 88 cal/mole). Equations 11*a* and 11*b* are approximations (but acceptable ones) of the experimental Eq. 10. No data exist for the θ values on the tablet matrix used, but it is expected to have a temperature dependence between that of an ionic and that of a covalently bonded surface.

The surface tension, γ, is dependent on temperature by the Ramsay–Shields rule (26):

$$\gamma(M/\rho)^{2/3} = k'(T_c - T - 6) \quad \text{(Eq. 12)}$$

where *M* is the molecular weight, ρ is the density, T_c is the critical temperature of the liquid, and k' is a constant (which equals about 2.1 for liquids that follow Trouton's rule). Since the critical temperature of water is high, γ is virtually temperature independent.

The dependence of viscosity on temperature is given by (25, 26):

$$\ln\eta = (4000/R)(1/T) + \ln\eta_0 \quad \text{(Eq. 13)}$$

This quantity is the only temperature-dependent term in Eq. 9, and it contributes substantially. Equation 9, when Eq. 13 is inserted, becomes:

$$\ln d = (6000/R)(1/T) + Q' \quad \text{(Eq. 14)}$$

where Q' is a nearly temperature-independent term. The slope predicted in Eq. 14 (3000) is on the same order as that found in Eq. 4. Therefore, the data in this case are not contradictory to the disintegration process as being penetration controlled.

REFERENCES

(1) J. Wagner, *J. Pharm. Sci.*, **58**, 1253 (1969).

(2) J. Wood, in "Abstracts of Papers Presented at the 113th Annual Meeting of the Academy of Pharmaceutical Sciences," American Pharmaceutical Association, Washington, D.C., 1974, p. 189.

(3) F. Langenbucher, *J. Pharm. Pharmacol.*, **24**, 979 (1972).

(4) I. Lippmann, in "Dissolution Technology," L. Leeson and J. T. Carstensen, Eds., Academy of Pharmaceutical Sciences, Washington, D.C., 1974, p. 193.

(5) K. G. Nelson and L. Y. Wang, *J. Pharm. Sci.*, **66**, 1758 (1977).

(6) *Ibid.*, **67**, 87 (1978).

(7) J. T. Carstensen, J. L. Wright, K. W. Blessel, and J. Sheridan, *J. Pharm. Sci.*, **67**, 48 (1978).

(8) *Ibid.*, **67**, 982 (1978).

(9) J. T. Carstensen, T. Y.-F. Lai, and V. K. Prasad, *J. Pharm. Sci.*, **67**, 1303 (1978).

(10) N. Kitamori and T. Shimamoto, *Chem. Pharm. Bull.*, **24**, 1789 (1976).

(11) N. Kitamori and K. Iga, *J. Pharm. Sci.*, **67**, 1436 (1978).

(12) P. Couvreur, Ph.D. thesis, Université Catholique de Louvain, Brussels, Belgium, 1975, p. 87.

(13) J. T. Ingram and W. Lowenthal, *J. Pharm. Sci.*, **55**, 614 (1966).

(14) *Ibid.*, **57**, 393 (1968).

(15) J. T. Carstensen and M. Patel, *J. Pharm. Sci.*, **64**, 1770 (1975).

(16) J. P. Cleave, *J. Pharm. Pharmacol.*, **17**, 698 (1965).

(17) H. Berry and C. W. Ridout, *ibid.*, **2**, 619 (1950).

(18) E. H. Washburn, *Phys. Rev.*, **17**, 273 (1921).

(19) H. Nogami, T. Nagai, and H. Uchida, *Chem. Pharm. Bull.*, **14**, 152 (1966).

(20) E. Nelson, D. Eppich, and J. T. Carstensen, *J. Pharm. Sci.*, **63**, 755 (1974).

(21) J. T. Carstensen, *ibid.*, **63**, 1 (1974).

(22) A. W. Adamson, "Physical Chemistry of Surfaces," 3rd ed., Wiley, New York, N.Y., 1976, p. 345.
(23) A. W. Neumann, *Z. Phys. Chem., Neue Folge*, **41**, 339 (1964).
(24) V. G. Stepanov, L. D. Volyak, and Y. V. Tarakov, *Zh. Fiz. Khim.*, **46**, 2397 (1972); through *Chem. Abstr.*, **77**, 169160c (1973).
(25) *Ibid.*, **49**, 2931 (1975); through *Chem. Abstr.*, **84**, 80161a (1976).
(26) W. J. Moore, "Physical Chemistry," 3rd ed., Prentice-Hall, Englewood Cliffs, N.J., 1963, p. 734.

ACKNOWLEDGMENTS

Supported by grants from Hoffmann-La Roche, Nutley, NJ 07110, and by Contract 223-76-3020 from the Food and Drug Administration.

Antitumor Agents XLI: Effects of Eupaformosanin on Nucleic Acid, Protein, and Anaerobic and Aerobic Glycolytic Metabolism of Ehrlich Ascites Cells

I. H. HALL ˣ, K. H. LEE, W. L. WILLIAMS, Jr., T. KIMURA, and T. HIRAYAMA

Received August 8, 1979, from the *Division of Medicinal Chemistry, School of Pharmacy, University of North Carolina, Chapel Hill, NC 27514.* Accepted for publication October 16, 1979.

Abstract □ The major effect of eupaformosanin as an antineoplastic agent on Ehrlich ascites cell metabolism was to inhibit deoxyribonucleic acid synthesis, specifically at deoxyribonucleic acid polymerase and thymidylate synthetase enzymatic sites. Both pyrimidine and purine systems of Ehrlich ascites were marginally inhibited. Ribonucleic acid synthesis and messenger and ribosomal polymerase activities also were suppressed. Cyclic adenosine monophosphate levels were increased significantly, which correlated with the drastic reduction of histone phosphorylation. Eupaformosanin also suppressed a number of glycolytic and Krebs cycle enzymes as well as oxidative phosphorylation *in vitro*. All of the inhibited enzymes are known thiol-bearing enzymes that can undergo a Michael-type addition with the α-methylene-γ-lactone moiety of eupaformosanin, as shown with other sesquiterpene lactones.

Keyphrases □ Antitumor agents—eupaformosanin, effect on nucleic acid, protein, and anaerobic and aerobic glycolytic metabolism, Ehrlich ascites cells □ Eupaformosanin—antitumor activity, effect on nucleic acid, protein, and anaerobic and aerobic glycolytic metabolism, Ehrlich ascites cells □ Deoxyribonucleic acid synthesis, inhibitors—eupaformosanin, effect on nucleic acid, protein, and anaerobic and aerobic glycolytic metabolism, Ehrlich ascites cells

A new germacranolide, eupaformosanin (I), has been isolated from the whole plant of *Eupatorium formosanum*, and its stereochemistry and physical characteristics were reported previously (1). As an antineoplastic agent, eupaformosanin is a potent inhibitor of Walker 256 carcinosarcoma cell proliferation at 2.5 mg/kg/day (T/C = 471) and of P-388 lymphocytic leukemia cell proliferation at 25 mg/kg/day (T/C = 147) (2). The effects of eupaformosanin on nucleic acid, chromatin protein, purine, pyrimidine, and protein metabolism, anaerobic and aerobic glycolysis, and oxidative phosphorylation of Ehrlich ascites tumor cells are reported here.

EXPERIMENTAL

Male CF_1 mice, ~30 g, were implanted intraperitoneally on Day 0 with 10^6 Ehrlich ascites tumor cells from donor mice housed in these laboratories. Eupaformosanin suspended by homogenization in 0.05% polysorbate 80–water was administered intraperitoneally at 25 mg/kg/day for 8 days to determine the inhibition of tumor growth (3). For the metabolic studies, mice were treated on Days 7–9 with a subacute dose of 0.25 mg ip. Animals were sacrificed on Day 10, and the ascites fluid was collected from the peritoneal cavity. *In vitro* metabolic studies were determined on untreated, harvested, Day 10 Ehrlich ascites cells. The number of tumor cells per milliliter and the 0.4% trypan blue uptake were determined with a hemocytometer (4).

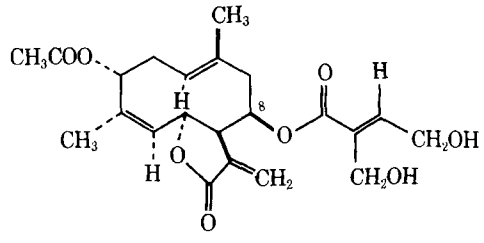

I

Incorporation of thymidine into deoxyribonucleic acid was determined by the method of Chae *et al.* (5). One hour prior to the animal sacrifice, 10 μCi of [^{14}C-*methyl*]-thymidine[1] (53.2 mCi/mmole) was injected intraperitoneally. The deoxyribonucleic acid was isolated, and the carbon-14 content was determined in two parts of toluene, one part of octoxynol, 0.4% 2,5-diphenyloxazole, and 0.01% 1,4-bis[2-(5-oxazolyl)]-benzene scintillation fluid and corrected for quenching. The deoxyribonucleic acid concentration was determined by UV spectrophotometry at 260 nm with calf thymus deoxyribonucleic acid as a standard.

Uridine incorporation into ribonucleic acid was determined in an analogous manner utilizing 10 μCi of 5-^{3}H-uridine (20.0 Ci/mmole). Ribonucleic acid was extracted by the method of Wilson *et al.* (6). Leucine incorporation into protein was determined by the method of Sartorelli (7) using 8 μCi of 1-^{14}C-leucine (54.4 mCi/mmole). The effect of eupaformosanin on 1-^{14}C-acetic acid (57.8 mCi/mmole) incorporation into cholesterol of Ehrlich ascites cells also was measured (8, 9).

Nuclear deoxyribonucleic acid polymerase activity was determined on isolated nuclei (10). The incubation medium was that of Sawada *et al.* (11), except that [^{3}H-*methyl*]-deoxyribothymidine-5′-triphosphate (53.1 mCi/mmole) was used and the insoluble nucleic acids were collected on glass fiber paper (GF/F) by vacuum suction. Deoxythymidine and deoxythymidylate monophosphate and diphosphate kinase activities were determined by the method of Maley and Ochoa (12), which is based on the disappearance of 0.1 μmole of reduced nicotinamide adenine dinucleotide at 340 nm.

Thymidine synthetase activity was assayed by the method of Kampf *et al.* (13) utilizing a postmitochondrial supernate (9000×*g* for 10 min) and 5 μCi of 5-^{3}H-deoxyuridine monophosphate (11 Ci/mmole). Mes-

[1] New England Nuclear was the source of all radioisotopes used in this study. Biochemical reagents were purchased from Sigma Chemical Co. and Calbiochem Co.

0022-3549/80/0300-0294$01.00/0